Theoretical and Measured PV System Output Using High-Resolution Data: Analysis and Comparative Performance

Nabeel I. Tawalbeh[1], and *Sadeq* A. Hamed[1,*]

[1]The University of Jordan, School of Engineering, Department of Electrical Engineering, Amman, Jordan 11942

Abstract. This paper presents a comparative performance analysis of a photovoltaic (PV) system using two distinct approaches; a mathematical model approach, based on standard test conditions and solar geometry using a cosine-squared function, and an experimental model approach, based on high resolution field measurements. The cosine-squared model was employed to simulate ideal clear-sky output based on actual sunrise and sunset times. AC power monitoring is conducted through five-minute interval basis across multiple seasons in 2023. The comparison is conducted on two large-scale PV subsystems (Car-Park-Mounted and Ground-Mounted subsystems) installed at the University of Jordan–Aqaba Branch. For this purpose, monthly energy yield, specific yield, and performance ratio are evaluated over a one-year period. Seasonal variations, efficiency trends, and potential losses due to real-world operating conditions were also identified. The results demonstrate that the Ground-Mounted system consistently outperformed the Car-Park-Mounted configuration, particularly under low-sun-angle or diffuse-light conditions, with efficiency differences, reaching up to 30%. Additionally, the analysis quantified the overestimation of energy in raw data, showing that daily energy can be inflated by nearly 9% if smoothing of raw measurements is not applied. These findings highlight the importance of combining theoretical modeling with high-resolution measurements to better interpret system performance, inform design decisions, and optimize operation under varying environmental conditions. The results not only validate the accuracy of the theoretical model but also highlight areas where environmental and operational factors cause significant deviations, providing actionable insights for PV system optimization in similar climatic contexts.

1 INTRODUCTION

The system under consideration is located in Aqaba, Jordan, a semi-arid region with high solar potential and pronounced seasonal irradiance variation. The site features two distinct PV layouts: a flat-roof Car Park system and a south-facing Ground-Mounted array. While numerous studies evaluate long-term PV performance using aggregated data, few focus on

* Corresponding author: hamed@ju.edu.jo

inverter-level trends at high temporal resolution or directly compare modeled and measured AC outputs. This study aims to address this gap. Photovoltaic (PV) systems have emerged as a cornerstone of sustainable energy generation due to their scalability, declining costs, and minimal environmental impact. As global deployment accelerates, ensuring consistent and efficient performance under real-world conditions becomes increasingly critical. Robust performance evaluation not only quantifies energy yield but also informs system design, operational planning, and long-term investment decisions [1], [2].

Conventional assessments of PV systems typically rely on daily or monthly summaries of energy yield and performance ratio. However, the widespread adoption of smart inverters and digital monitoring platforms has made high-resolution data (e.g., five-minute intervals) increasingly accessible [3]. This enables deeper understanding of system behavior, leading to uncovering short-term dynamics such as shading events, cloud transients and inverter response, which are often obscured in lower-resolution summaries. Recent studies underscore the value of high-frequency data for diagnosing performance anomalies, tracking soiling and degradation, and improving fault detection [4], [5].

This paper presents a comparative analysis of theoretical and measured PV system output using high-resolution inverter data. A cosine-squared irradiance model is used to simulate ideal clear-sky AC power curves [6], [7], with a moving average filter is applied to extract smoothed trends from the measured data [1]. By comparing these profiles under varying seasonal and weather conditions, the analysis quantifies deviations caused by layout geometry, shading, and environmental effects. The case study reported in this paper focuses on a dual-layout PV installation in southern Jordan, comprising both Car Park and Ground-Mounted arrays. Such hybrid configurations are increasingly common in urban and institutional settings, yet their relative performance under identical climatic conditions remains underexplored [8]. The analysis spans four representative months—January, April, July, and August 2023—covering system efficiency, specific yield trends (ranging from 3.1 to 6.4 kWh/kWp/day), and daily energy output. The findings highlight the influence of array design and data resolution on the performance assessment.

The remainder of this paper are organized as follows: Section II outlines the system specifications and layout, Section III provides electrical design considerations, Section IV details the modeling approach and data processing steps, Section V presents the key findings, including comparative performance metrics, and Section VI concludes with a summary and suggestions for future work.

2 SYSTEM CONFIGURATION

The photovoltaic (PV) system investigated in this study consists of two interconnected subsystems: a Car Park (CP) installation and a Ground-Mounted (GM) installation. Although both utilize identical PV modules and inverters, they differ in layout, tilt angle, azimuth orientation, and exposure to shading. Together, the systems offer a combined DC capacity of 500.5 kWp and are monitored via a centralized Solar-Log Platform. For consistency, inverters are labeled INV1 to INV23; with INV1–INV8 correspond to the Car Park system, and INV9–INV23 are assigned to the Ground-Mounted system. This labeling is maintained throughout all figures and analysis in this paper.

2.1 Car Park (CP) PV System

The Car Park system is mounted on parking canopy structures, serving a dual purpose of vehicle shading and solar power generation. PV modules are installed at a tilt angle of 5° with an azimuth of -71°. This subsystem includes 520 multi-crystalline modules, each rated at 325 W with a module efficiency of 16.77%, yielding a total nominal DC capacity of 169 kWp.

Eight three-phase inverters (INV1–INV8), model Kaco Blueplanet 20.0 TL3 INT, each rated at 20 kW, are used in this layout. Each inverter is equipped with two MPPT inputs and connects to four PV strings (two per MPPT), with 17 modules per string. This configuration ensures balanced input and facilitates effective monitoring and fault isolation.

2.2 Ground-Mounted (GM) PV System

The Ground-Mounted system is installed on fixed galvanized steel frames in an open field, providing optimal solar exposure. Modules are mounted at a tilt angle of 22°, with azimuth angles of −71° and 19°, depending on the row orientation. This array includes 1020 identical modules, delivering a total nominal DC capacity of 331.5 kWp. The GM system is supported by fifteen inverters (INV9–INV23), identical in model and configuration to those used in the CP system. Each inverter connects to four strings of 17 modules via two MPPT inputs, following the same electrical layout as the Car Park system.

3 ELECTRICAL DESIGN CONSIDERATIONS

Both PV subsystems follow a uniform electrical layout. Each inverter receives input from two MPPT channels, each handling two PV strings of 17 modules. Each module has a rated maximum power point voltage of $V_{mp,module}$ = 37.49 V under standard test conditions (STC, 25°C). The resulting string voltage at STC is:

$$V_{mp} = 17 \times V_{mp,module} = 17 \times 37.49 = 637.33\,V \quad (1)$$

To account for temperature effects, the string voltage at a given module temperature T is estimated using:

$$V(T) = V_{mp} \times (1 + \gamma \times (T - 25)) \quad (2)$$

Where γ is the temperature coefficient, that is equal to (−0.003/°C). These values represent the expected DC string voltage under different module temperature conditions, adjusted from the rated maximum power point voltage at STC. Example values include:

- at T = 80°C module temperature: $V(80°C)$ = 637.33 × (1 − 0.0033 × 55) = 521.65 V
- at T = 0°C module temperature: $V(0°C)$ = 637.33 × (1+0.0033 × 25) = 689.90 V

The open-circuit voltage per moduleis $V_{oc,module}$ = 46.48 V, giving a string open-circuit voltage of:

$$V_{oc} = 17 \times V_{oc,module} = 17 \times 46.48\ V = 790.16\ V \quad (3)$$

These values fall within the inverters' MPPT tracking range of 515–800 V, as specified in the manufacturer's datasheet [9]. This remains safely below the inverter's maximum DC input limit of 1000 V.

AC outputs from both systems are routed through separate distribution panels (MDB–CP and MDB–GM) and integrated into the facility's main electrical infrastructure. Both PV subsystems share a standardized string configuration and inverter layout, but differ in mounting type, tilt angle, and shading susceptibility. A summary of these design characteristics of both systems, including inverter and PV moule numbers, total DC power capacity, inverter rated power, PV mounting type, Tilt angle and azimuth, shading, PV string configuration, inverter MPPT inputs and voltage range, is provided in Table (1), Appendix (1).

4 DATA AND METHODOLOGY

All inverters are monitored by a Solar-Log data acquisition system at five-minute intervals. This section outlines the modeling of theoretical power output, smoothing of raw measurements, and methodology for performance comparison.

4.1 Theoretical Power Curve Approximation

To approximate ideal inverter output under clear sky conditions, a cosine-squared function, centered around solar noon, is adopted. This bell-shaped curve mimics the symmetrical irradiance profile expected on unobstructed sunny days [6], [7]. The cosine-squared formulation is chosen because it approximates the expected irradiance pattern on a cloudless day, assuming symmetric solar elevation around noon with no shading or atmospheric variation. This model is commonly used in PV literature as a clear-sky reference profile. Theoretical power is then given as:

$$P_{theoritical}(t) = P_{rated}\left(\frac{\pi(t-t_{noon})}{\Delta t}\right) \quad (4)$$

where:

- P_{rated} is the nominal inverter AC power (i.e., 20 kW),
- t is the time in decimal hours,
- t_{noon} is the midpoint between sunrise and sunset, and
- Δt is the daylight duration in hours.

Implementation Example:

For January 16, 2023, inverter output was observed between 07:40 and 18:05 hours, based on the first and last non-zero values in the AC power data. These correspond to $t_{sunrise}$ = 7.6667*and* t_{sunset} = 18.0833, yielding a daylight duration of Δt = 10.4166 hours. The effective solar noon t_{noon} is then calculated as: $t_{noon} = \frac{7.6667+18.0833}{2}$.

These actual values were used in the cosine-squared formulation to generate a theoretical power profile aligned with the real operating conditions for the selected day, bearing in mind that:

$$P_{theoretical}(t) = 0 \text{ for } t < t\text{sunrise and } t > t\text{sunset} \quad (5)$$

The total theoretical energy yield for the day is then calculated by means of:

$$E_{theoritical} = \int_{t_{surise}}^{t_{sunset}} P_{theoritical}(t)dt \quad (6)$$

In practice, since the data is sampled at discrete 5-minute intervals, this integral is approximated using a finite summation:

$$E_{theoritical} = \sum_{i=1}^{N} P_{theoritical}(t_i) \times \Delta t \quad (7)$$

Where $\Delta t = \frac{5}{60} = 0.0833$ hours is the time step between measurements, and N is the total number of valid power samples during the day. The result is expressed in kilowatt-hours (kWh). Eq. (7) gives the ideal daily AC energy output under perfect clear-sky conditions, assuming that the inverters operate without clipping or losses.

To validate the proposed model, theoretical and measured AC power were compared on a cloudy winter day (January 14, 2023). Figure 5 presents results for INV1 (Car Park) and INV10 (Ground-Mounted). The theoretical daily energy was estimated as $E_{\text{theoretical}}$ = 105.00

kWh. The measured daily energy of INV1 = $E_{\text{measured,INV1}} = 66.24\ kWh$ and that of INV10 = $E_{\text{measured,INV10}} = 91.16\ kWh$. The difference between theoretical and measured values highlights the effect of system geometry and shading, particularly under low-irradiance conditions.

4.2 The Role of Smoothed Power in daily Performance Comparison

The AC output power $P_{ac\ of}$ the PV system, recorded in five-minute intervals captures, high frequency variability caused by cloud movement, rapid irradiance changes, and momentary shading. While this granularity is valuable for fault detection and transient behavior analysis, it can obscure the daily performance pattern expected under clear-sky conditions. To uncover the underlying trend, a 12-point moving average filter, equivalent to one hour of data, is applied to the raw power signal. The smoothing process is described by:

$$P_{smoothed}(t_k) = \frac{1}{N}\sum_{i=0}^{N-1} P_{raw}(t_{k-i}) \tag{8}$$

Where $P_{\text{raw}}(t_k)$ is the measured AC power at time step t_k, $N = 12$ denotes the smoothing window size, and i is a discrete-time index. This smoothing technique helps suppress short term fluctuations and reveals the expected bell- shaped curve that characterizes solar generation on clear days. It also facilitates consistent comparison with theoretical cosine-squared models and aligns with IEC 61724 recommendations for PV system monitoring [1].

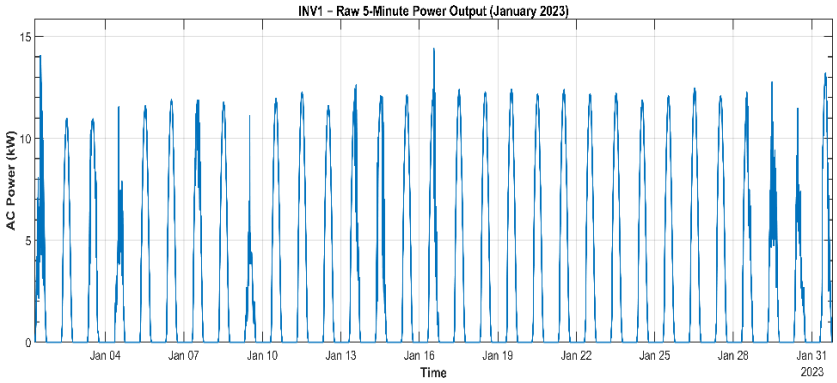

Fig. 1. Raw AC power output of INV1 (5-minute resolution) during January 2023.

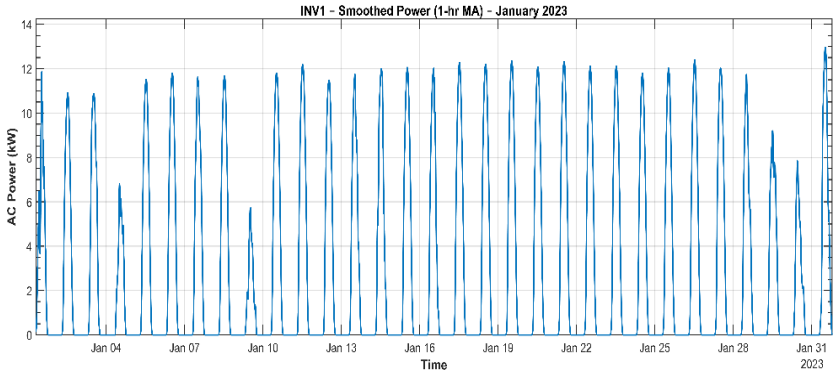

Fig. 2. Smoothed AC power profile of INV1 using a 1-hour moving average (January 2023).

Progression of Insight from Raw to Filtered Data

To visualize the impact of filtering, Figs. 1 and 2 show the raw and smoothed power profiles of INV1 respectively for the entire month of January 2023. From these two figures, it can be realized that the smoothed profile makes the daily patterns more distinct, with a reduction of the clutter caused by transient events.

Figure (3) shows how does the smoothing process affect the single-day behavior, by comparing raw and smoothed curves for two representative days; January 8 and January 28. It can be shown that the smoothing process tends to eliminates spikes caused by rapid irradiance changes, and highlights the underlying performance curve.

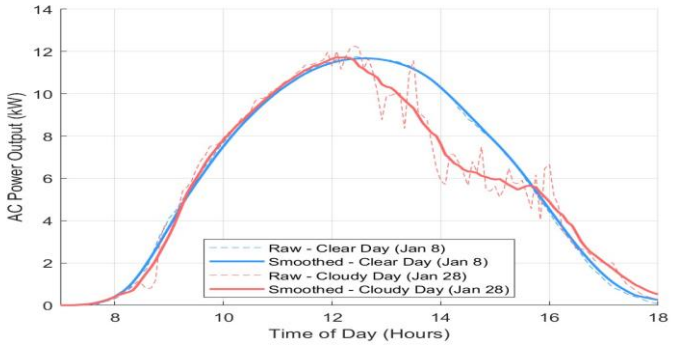

Fig. 3. Raw vs. smoothed AC power output on January 8 and 28, 2023 (Car Park Inverter 1).

Variations of the raw and smoothed power outputs of INV1 and INV10 on day January 14, 2023 are shown in Fig.4. Calculation of the generated energy of both curves yields that the raw energy is 109.2 kWh, while the smoothed is 100.0 kWh; implying a discrepancy of 9%. This overestimation is due to transient power spikes in the raw data.

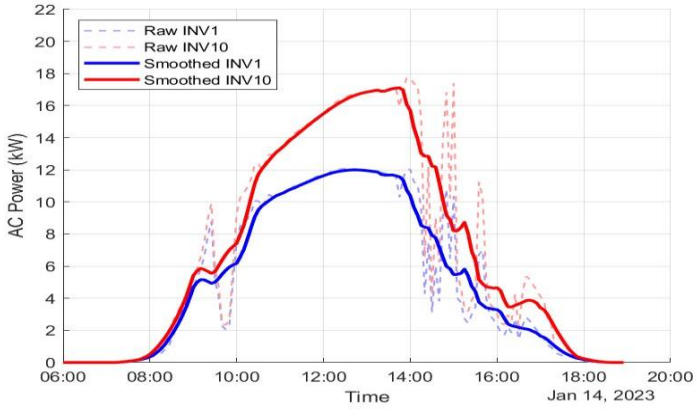

Fig. 4. Raw and smoothed AC power for INV1 and INV10 on January 14, 2023.

Theoretical comparison between the output power of the developed theoretical model and the measured power if INV1 and INV10, is shown in Fig. 5. It can be seen that the use of filtered data for comparing measured output to that of the theoretical model is highly required since it enhances consistency and avoid overestimation. As illustrated by the figure, the smoothed power curve aligns well with the theoretical cosine-squared profile under stable irradiance.

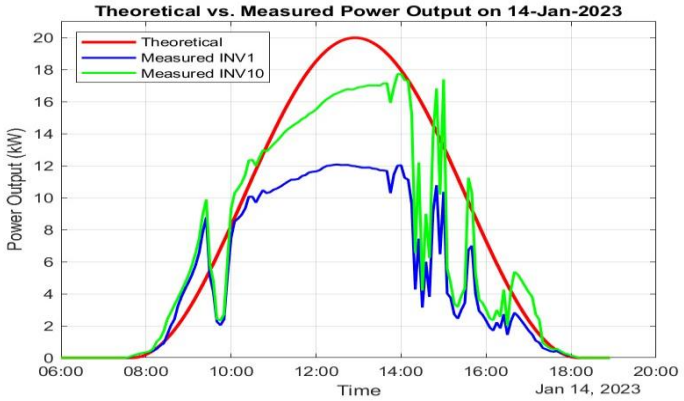

Fig. 5. Theoretical vs. measured AC power on January 14, 2023 for INV1 and INV10.

5 RESULTS AND DISCUSSION

This section presents the performance analysis of the PV system in accordance with IEC 61724 standards for system monitoring [1], using high resolution data acquired via the Solar-Log Platform [3].

5.1 Specific Yield Trends

Figure 6 shows the monthly energy yield and specific yield of the PV system under consideration in year 2023, where a total of 899.2 MWh was generated. Knowing that the installed capacity of the system is 460 kWp, the annual specific yield is 1954.8 kWh/kWp.

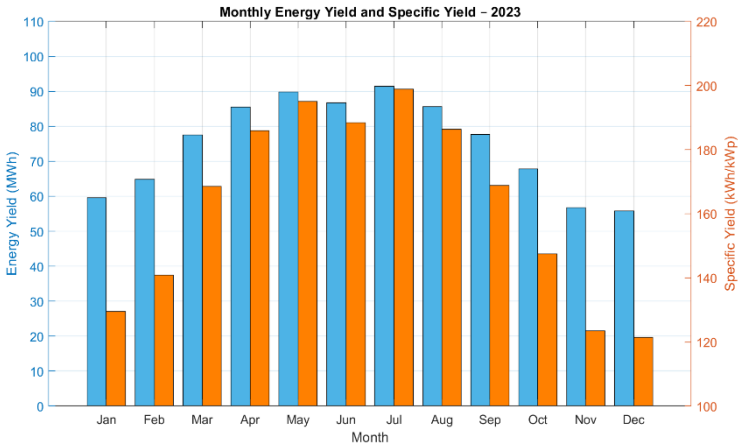

Fig. 6. Monthly energy yield and specific yield of the PV system in 2023.

This is a key indicator of site productivity normalized by system size. Daily specific yields exhibited clear seasonal variation, ranging from 3.1 kWh/kWp/day on overcast winter days to 6.4 kWh/kWp/day during peak summer performance. Typical values ranged between 4.2 and 5.9 kWh/kWp/day, depending on irradiance conditions. As shown by the figure, the

system followed the expected seasonal trends, with a maximum yields during e summer months and reduced output in winter.

5.2 Comparative System Behavior on Cloudy Days

To evaluate the impact of mounting configuration under diffuse irradiance, overcast days in January 2023 were identified by visual inspection of the AC power profile. January 16 was selected as a representative example. On this day, the Car Park inverter, characterized by a lower tilt angle and susceptibility to shading, exhibited greater short-term variability and more pronounced power dips. In contrast, the Ground-Mounted inverter delivered smoother and more stable output, supported by its optimal tilt and unshaded location that enhances diffuse irradiance capture. These results emphasize the influence of geometry and placement on energy capture during nonideal weather conditions. As introduced earlier in Section IV, this behavior is illustrated in Fig.7.

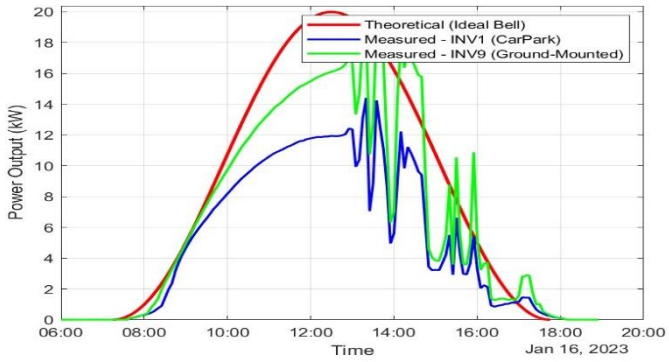

Fig. 7. Theoretical vs measured AC power of INV1 and INV10 on January 16, 2023.

5.3 System Efficiency Comparison in January

To quantitatively assess wintertime performance, Figure 8 shows the daily average group efficiency of the Car Park and Ground-Mounted systems during January 2023. As can be noticed, Ground-Mounted array consistently outperformed the Car Park one. Figure 9 extends this comparison by illustrating the GM-averaged daily efficiencies throughout three representative months (January, April and July). August data, which is almost closely mirrors of July's trend, is excluded.

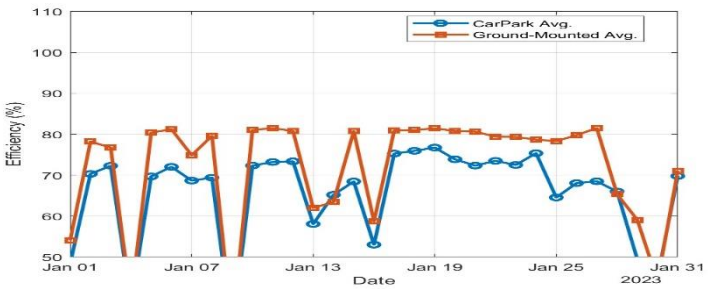

(a) January 2023

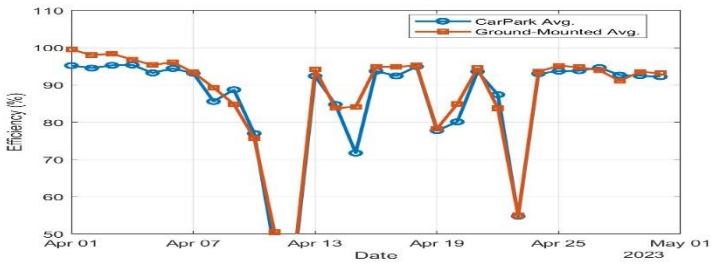

(b) April 2023

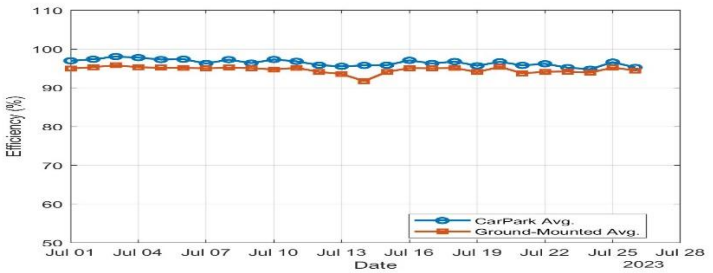

(c) July 2023.

Fig. 8. Daily average energy efficiency of Car Park and Ground-Mounted systems

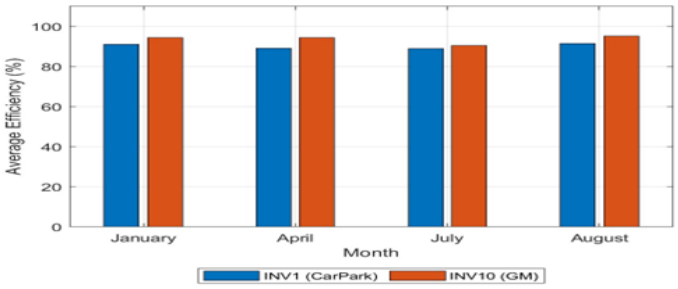

Fig. 9. Monthly average efficiency comparison between INV1 and INV10.

6 CONCLUSIONS

This study presented a comparative analysis and performance of the theoretical and measured outcomes of the PV system using high-resolution inverter data, obtained from a dual-layout (Car Park and Ground-Mounted) installation installed in southern Jordan. A cosine-squared function was employed to approximate ideal clear-sky power output, providing reliable reference baseline for performance assessment and system optimization. The Theoretically calculated output power was compared with the measured 5-minute interval data in order to evaluate the system behavior under varying weather and seasonal conditions.

The results revealed that the Ground-Mounted system consistently outperformed the Car Park array in both energy yield and efficiency, particularly under clear-sky and diffuse-light conditions. Daily specific yield ranged from 3.1 to 6.4 kWh/kWp/day, with peak monthly outputs observed in summer months. The Car Park system exhibited greater variability, primarily due to its low tilt angle and exposure to structural shading, while the Ground-Mounted array demonstrated more stable and efficient performance.

These findings highlight the substantial influence of array layout and physical configuration on PV system effectiveness. Theoretical modeling proved to be a valuable diagnostic tool for benchmarking and identifying deviations from ideal output conditions. High-resolution monitoring enabled detailed performance evaluation, capturing short-term fluctuations and shading-induced losses that would be missed in lower-resolution datasets.

Overall, the Ground-Mounted system achieved an overall 10–15% higher average efficiency, with up to 30% advantage under cloudy conditions. These outcomes reinforce the critical role of tilt angle, orientation, and shading in PV system design, especially during low sun-angle months.

Future work is expected to focus on integrating onsite irradiance measurements, extending the analysis to full-year efficiency trends, and exploring certain approaches to classify performance patterns or detect inverter-level anomalies.

Acknowledgments

The authors thank the technical staff and the facility management team at KAWAR Energy Company in Jordan for their support in accessing and maintaining the PV system data used in this study.

REFERENCES

1. International Electrotechnical Commission, *Photovoltaic System Performance Monitoring – Guidelines for Measurement, Data Exchange and Analysis,* IEC Standard 61724-1, 2017.
2. International Energy Agency (IEA) PVPS Task 13, *Performance and Reliability of Photovoltaic Systems.* [Online]. Available: https://iea-pvps.org. Accessed: Mar. 2023.
3. Solar-Log GmbH, *Solar-Log Monitoring Portal.* [Online]. Available: https://www.solar-log.com. Accessed: Mar. 2023.
4. K. Yamamoto, K. Nishioka, and K. Kurokawa, "Real-time performance monitoring of PV systems using high-resolution data," *Renewable Energy,* vol. 146, pp. 1383–1390, 2020.
5. J. Keller, N. Hostettler, and B. Bletterie, "High-frequency inverter data for enhanced PV diagnostics and fault detection," *Solar Energy,* vol. 180, pp. 224–233, 2019.
6. J. A. Duffie and W. A. Beckman, *Solar Engineering of Thermal Processes,* 4th ed. Hoboken, NJ, USA: John Wiley & Sons, 2013.
7. National Renewable Energy Laboratory (NREL), *Clear-Sky Solar Radiation Models.* [Online]. Available: https://www.nrel.gov. Accessed: Mar. 2023.
8. M. S. S. Abujazar, M. Y. Othman, M. H. Ruslan, and K. Sopian, "Evaluation of grid-connected photovoltaic performance in Jordan: A comparative layout analysis," *Renewable and Sustainable Energy Reviews,* vol. 132, p. 110051, 2020.
9. KACO new energy GmbH, *Blueplanet 20.0 TL3 INT – Technical Data Sheet,* 2022. [Online]. Available: https://www.kaco-newenergy.com. Accessed: Mar. 2023.

APPENDIX (1)

Table 1. Summary of PV System Electrical Characteristics as Described in Section III

Parameter	***Car Park System (CP)***	***Ground-Mounted System (GM)***
Inverter Numbers	*INV1–INV8*	*INV9–INV23*
Number of Modules	*520*	*1020*
Total DC Capacity	*169 kWp*	*331.5 kWp*
Rated Power per Inverter	*20 kW*	*20 kW*
Mounting Type	*Rooftop over parking canopy*	*Ground-mounted steel frames*

Tilt Angle	*5°*	*22°*
Azimuth	*−71°*	*−71° and 19°*
Shading Susceptibility	*High (due to vehicles and nearby structures)*	*Low (open field exposure)*
PV String Configuration	*4 strings × 17 modules*	*4 strings × 17 modules*
Inverter MPPT Inputs	*2 per inverter*	*2 per inverter*
Voltage Range (MPPT)	*515–800 V*	*515–800 V*